ELSEVIER

Coordination Chemistry Reviews
216–217 (2001) 173–194

COORDINATION CHEMISTRY REVIEWS

www.elsevier.com/locate/ccr

Molecular design of luminescent dinuclear gold(I) thiolate complexes: from fundamentals to chemosensing

Vivian Wing-Wah Yam *, Chui-Ling Chan, Chi-Kwan Li, Keith Man-Chung Wong

Department of Chemistry, The University of Hong Kong, Pokfulam Road, Hong Kong, People's Republic of China

Received 8 August 2000; received in revised form 21 November 2000; accepted 19 December 2000

Contents

* Corresponding author. Tel.: +852-2859-2153; fax: +852-2857-1586.
E-mail address: wwyam@hku.hk (V.W.-W. Yam).

0010-8545/01/$ - see front matter © 2001 Elsevier Science B.V. All rights reserved.
PII: S0010-8545(01)00310-1

Abstract

A number of dinuclear gold(I) phosphine thiolates have been synthesized and characterized. Detailed spectroscopic and luminescence studies have provided a fundamental understanding on their spectroscopic origins, which serves as the basis for the design of versatile spectrochemical and luminescence chemosensors as well as molecular optoelectronic 'on-off' switching devices based on the switching on and off of weak metal···metal interactions using the dinuclear gold(I) phosphine thiolate as the basic building block. The binding characteristics have been studied by both UV–vis and emission spectroscopic measurements, and the identities of the ion-bound species have been confirmed by electrospray-ionization mass spectrometric studies. © 2001 Elsevier Science B.V. All rights reserved.

Keywords: Gold(I); Thiolate; Gold–gold interaction; Emission; Crown ether; Chemosensing; Spectrochemical; Luminescence signalling; Ion probe

1. Introduction

Polynuclear metal complexes, particularly those of d^{10} electronic configuration, have attracted much attention in view of their intriguing structural diversity [1–22] and the ability of a number of them to exhibit rich luminescence properties [2–19,23–34]. The first report on the luminescence properties of d^{10} metal complex systems dated back to 1970 when Dori and coworkers noted the luminescence behaviour of d^{10} metal phosphine complexes of copper(I), silver(I), gold(I), nickel(0), palladium(0) and platinum(0) [33]. Later works by a number of groups [2,3,5–7,9,18,19,24–31], mainly pioneered by the works of Gray and coworkers [24], have established the importance of metal–metal interactions in the origin of the luminescence behaviour. In fact, polynuclear d^{10} metal complexes are also interesting from a structural point of view, in which short metal–metal distances are often observed in many of these complexes. This is particularly obvious in gold(I) metal complexes, where short Au···Au contacts are often observed as a result of the relativistic effects. This phenomenon has been termed *aurophilicity* by Schmidbaur [35]. An understanding of the bonding interactions between closed-shell d^{10} metal centres has attracted much attention [1,22,34–36].

Luminescent gold(I) thiolates containing phosphine ligands [6,21,30] represent a class of polynuclear d^{10} metal complexes whose excited states are also related to metal–metal interactions. Fackler and coworkers illustrated the importance of metal–metal separation on the photophysical properties of this class of complexes, in which the emission energies are found to be a function of both gold–gold interactions and the nature of the thiolates [6]. The solid-state emissions of a series

of mononuclear gold(I) thiolate complexes [L–Au–SR] with phosphine ligands L at 77 K occur over a wide energy range (413–702 nm). The origin of the emission has been ascribed to a ligand-to-metal charge transfer (LMCT) [$RS^- \rightarrow Au$] triplet state. Lower emission energy is observed for those with electron-donating substituents on the phenyl ring of the thiolate ligand and those with short intermolecular Au···Au distances. The excited state for those complexes with short Au···Au contacts has been suggested as ligand-to-metal–metal charge-transfer (LMMCT) in nature. In view of our recent interest in the luminescence behaviour of polynuclear d^{10} and d^8 metal complexes containing chalcogen ligands [11–15,37], a series of luminescent dinuclear gold(I) thiolates have recently been synthesized in our laboratory [10] employing the bis(diphenylphosphino)alkyl- and aryl-amine ligands, $Ph_2PN(R)PPh_2$. Bis(diphosphino)amine-type ligands have proved to be very versatile because substituents on both phosphorus and nitrogen atoms can be varied with attendant changes in the P–N–P bond angle and the conformation around the phosphorus centres [38–40]. The electronic properties of the complexes could be readily tuned through a variation of the R substituent on nitrogen. The effect of variation in the diphosphine has also been probed by the use of 1,8-bis(dicyclohexylphosphino)naphthalene (dcpn) as the bridging ligand. It is believed that through a systematic variation of the diphosphine ligands and the thiolate groups, further insight into the origin of the emission could be obtained. It is also anticipated that the present dinuclear gold(I) thiolate building block based on the switching on and off of weak metal···metal interactions, would serve as an ideal candidate for the design of spectrochemical and luminescence chemosensors as well as molecular optoelectronic 'on-off' switching devices [28].

2. Experimental

2.1. Reagents and materials

Potassium tetrachloroaurate(III) was purchased from Strem Chemicals Inc. *p*-Thiocresol, 4-fluorothiophenol, 4-chlorothiophenol and 3,4-dimethoxythiophenol were purchased from Lancaster Synthesis Ltd. The ligands bis(diphenylphosphino)cyclohexylamine [41–43], bis(diphenylphosphino)aniline [41–43], bis-(diphenylphosphino)-*n*-propylamine [41–43], bis(diphenylphosphino)-*i*-propylamine [41–43], 1,8-bis(dicyclohexylphosphino)naphthalene [44], and 4′-mercaptomonobenzo-15-crown-5 [45] were synthesized by published procedures. $[Au_2(Ph_2PN(R)PPh_2)Cl_2]$ and $[Au_2(dcpn)Cl_2]$ were prepared by modification of procedures published previously [27,46]. $[Au_2(Ph_2PN(R)PPh_2)(SR')_2]$ [$R = C_6H_{11}$, $R' = C_6H_4F$-4 (**1**), C_6H_4Cl-4 (**2**), $C_6H_4CH_3$-4 (**3**); $R = Ph$, $R' = C_6H_4CH_3$-4 (**4**); $R = CH_2CH_2CH_3$, $R' = C_6H_4CH_3$-4 (**5**); $R = CH(CH_3)_2$, $R' = C_6H_4CH_3$-4 (**6**)] were prepared according to procedures reported previously [10]. All solvents were purified and distilled by standard procedures before use. All other reagents were of analytical grade and used as received.

All reactions were carried out under anhydrous and anaerobic conditions using standard Schlenk techniques.

2.2. Synthesis of gold(I) complexes

2.2.1. $[Au_2(Ph_2PN(C_6H_{11})PPh_2)(S\text{-benzo-15-crown-5})_2]$ (7)

The procedure was similar to that for $[Au_2(Ph_2PN(R)PPh_2)(SR')_2]$ [10]. To a solution of $[Au_2(Ph_2PN(C_6H_{11})PPh_2)Cl_2]$ (100 mg, 0.11 mmol) in dichloromethane (15 ml) was added an ethanolic solution (1 ml) of 4′-mercaptomonobenzo-15-crown-5 (64 mg, 0.21 mmol) and triethylamine (33 μl, 0.24 mmol). The reaction mixture was stirred at room temperature (r.t.) for 30 min, after which the solvent was removed under reduced pressure. The yellow residue was then recrystallized from benzene–dichloromethane–hexane to give a yellow solid of **7** (120 mg, 0.08 mmol, 77% yield). ^{1}H-NMR (300 MHz, $CDCl_3$, 298 K, relative to Me_4Si): δ 0.78–1.48 (m, 10 H, cyclohexyl), 3.40–3.55 (m, 1 H, NCH of cyclohexyl), 3.70–4.08 (m, 32 H, CH_2 of crown ether) 6.48 (m, 2 H, Ar–H), 6.80–6.92 (m, 4 H, Ar–H) and 7.40–7.92 (m, 20 H, PPh_2). Positive-ion FAB mass spectrum: m/z 1459 $\{M^+\}$. Elemental analysis: Anal. Found: C, 46.36; H, 4.72; N, 0.92. Calc. for $C_{58}H_{69}Au_2NO_{10}P_2S_2{\cdot}0.75CH_2Cl_2$: C, 46.32; H, 4.63; N, 0.92%.

2.2.2. $[Au_2(Ph_2PN(C_6H_{11})PPh_2)\{SC_6H_3(OMe)_2\text{-}3,4\}_2]$ (8)

The procedure was similar to that for **7** except 3,4-dimethoxythiophenol (37 mg, 0.21 mmol) was used in place of 4′-mercaptomonobenzo-15-crown-5. Recrystallization of the crude product gave **8** as a yellow solid (98 mg, 0.08 mmol, 76% yield). ^{1}H-NMR (300 MHz, $CDCl_3$, 298 K, relative to Me_4Si): δ 0.74–1.48 (m, 10 H, cyclohexyl), 3.40–3.55 (m, 1 H, NCH of cyclohexyl), 3.65 (s, 6 H, OCH_3), 3.75 (s, 6 H, OCH_3) 6.52 (m, 2 H, Ar–H), 6.80–6.94 (m, 4 H, Ar–H) and 7.40–7.84 (m, 20 H, PPh_2). Positive-ion FAB mass spectrum: m/z 1200 $\{M^+\}$. Elemental analysis: Anal. Found: C, 46.05; H, 4.13; N, 1.38. Calc. for $C_{46}H_{49}Au_2NO_4P_2S_2$: C, 46.06; H, 4.09; N, 1.17%.

2.2.3. $[Au_2(Ph_2PN(Ph)PPh_2)(S\text{-benzo-15-crown-5})_2]$ (9)

The procedure was similar to that for **7** except that $[Au_2(Ph_2PN(Ph)PPh_2)Cl_2]$ (102 mg, 0.11 mmol) was used in place of $[Au_2(Ph_2PN(C_6H_{11})PPh_2)Cl_2]$. Recrystallization of the crude product gave **9** as a yellow solid (124 mg, 0.09 mmol, 79% yield). ^{1}H-NMR (300 MHz, $CDCl_3$, 298 K, relative to Me_4Si): δ 3.72–4.08 (m, 32 H, CH_2 of crown ether), 6.32 (dd, 2 H, NPh), 6.52 (dd, 2 H, Ar–H), 6.74 (dd, 2 H, NPh), 6.95–7.00 (m, 1 H, Ph proton *para* to N of NPh; 2 H, Ar–H), 7.08 (m, 2 H, Ar–H) and 7.32–7.66 (m, 20 H, PPh_2). Positive-ion FAB mass spectrum: m/z 1154 $\{[M-S\text{-benzo-15-crown-5}]^+\}$. Elemental analysis: Anal. Found: C, 46.85; H, 4.45; N, 0.99. Calc. for $C_{58}H_{63}Au_2NO_{10}P_2S_2{\cdot}0.5CH_2Cl_2$: C, 46.96; H, 4.21; N, 0.94%.

2.2.4. $[Au_2(Ph_2PN(Ph)PPh_2)\{SC_6H_3(OMe)_2\text{-}3,4\}_2]$ (10)

The procedure was similar to that for **9** except 3,4-dimethoxythiophenol (37 mg, 0.21 mmol) was used in place of 4′-mercaptomonobenzo-15-crown-5. Recrystalliza-

tion of the crude product gave **10** as a yellow solid (98 mg, 0.08 mmol, 76% yield). ^{1}H-NMR (300 MHz, $CDCl_3$, 298 K, relative to Me_4Si): δ 3.70 (s, 6 H, OCH_3), 3.80 (s, 6 H, OCH_3), 6.32 (dd, 2 H, NPh), 6.50 (dd, 2 H, Ar–H), 6.70 (dd, 2 H, NPh), 6.85–7.00 (m, 1 H, Ph proton *para* to N of NPh; 2 H, Ar–H), 7.08 (m, 2 H, Ar–H) and 7.32–7.68 (m, 20 H, PPh_2). Positive-ion FAB mass spectrum: m/z 1193 $\{M^+\}$. Elemental analysis: Anal. Found: C, 45.23; H, 3.49; N, 0.96. Calc. for $C_{46}H_{43}Au_2NO_4P_2S_2 \cdot 0.5CH_2Cl_2$: C, 45.19; H, 3.56; N, 1.13%.

2.2.5. *[Au_2($Ph_2PN(^nPr)PPh_2$)(S-benzo-15-crown-5)$_2$]* (**11**)

The procedure was similar to that for **7** except that [Au_2($Ph_2PN(^nPr)PPh_2$)Cl_2] (98 mg, 0.11 mmol) was used in place of [Au_2($Ph_2PN(C_6H_{11})PPh_2$)Cl_2]. Recrystallization of the crude product gave **11** as a yellow solid (124 mg, 0.09 mmol, 80% yield). ^{1}H-NMR (300 MHz, $CDCl_3$, 298 K, relative to Me_4Si): δ 0.16 (t, 3 H, Me group of *n*-propyl), 0.68–0.80 (m, 2 H, CH_2 of *n*-propyl), 2.72–2.88 (m, 2 H, NCH_2), 3.60–4.18 (m, 32 H, CH_2 of crown ether), 6.42 (m, 2 H, Ar–H), 6.78–6.98 (m, 4 H, Ar–H) and 7.44–7.80 (m, 20 H, PPh_2). Positive-ion FAB mass spectrum: m/z 1121 {[M–S-benzo-15-crown-5]$^+$}. Elemental analysis: Anal. Found: C, 45.43; H, 4.55; N, 0.94. Calc. for $C_{55}H_{65}Au_2NO_{10}P_2S_2 \cdot 0.5CH_2Cl_2$: C, 45.59; H, 4.58; N 0.96%.

2.2.6. *[Au_2($Ph_2PN(^nPr)PPh_2$){$SC_6H_3(OMe)_2$-3,4}$_2$]* (**12**)

The procedure was similar to that for **11** except 3,4-dimethoxythiophenol (37 mg, 0.21 mmol) was used in place of 4′-mercaptomonobenzo-15-crown-5. Recrystallization of the crude product gave **12** as a yellow solid (102 mg, 0.09 mmol, 79% yield). ^{1}H-NMR (300 MHz, $CDCl_3$, 298 K, relative to Me_4Si): δ 0.16 (t, 3 H, Me group of *n*-propyl), 0.68–0.80 (m, 2 H, CH_2 of *n*-propyl), 2.72–2.88 (m, 2 H, NCH_2), 3.72 (s, 6 H, OCH_3), 3.80 (s, 6 H, OCH_3), 6.42 (m, 2 H, Ar–H), 6.74–6.98 (m, 4 H, Ar–H) and 7.46–7.80 (m, 20 H, PPh_2). Positive-ion FAB mass spectrum: m/z 1159 $\{M^+\}$. Elemental analysis: Anal. Found: C, 44.26; H, 3.84; N, 1.11. Calc. for $C_{43}H_{45}Au_2NO_4P_2S_2$: C, 44.54; H, 3.88; N, 1.21%.

2.2.7. *[Au_2(dcpn)(SC_6H_4F-*p*)$_2$]* (**13**)

The procedure was similar to that for [Au_2($Ph_2PN(R)PPh_2$)(SR')$_2$] [15]. To a solution of [Au_2(dcpn)Cl_2] (104 mg, 0.11 mmol) in dichloromethane (15 cm^3) was added an ethanolic solution (1 cm^3) of 4-fluorothiophenol (27 mg, 0.21 mmol) and triethylamine (33 μl, 0.24 mmol). The reaction mixture was stirred at r.t. for 30 min, after which the solvent was removed under reduced pressure. The yellow residue was then recrystallized from benzene–dichloromethane–hexane to give orange crystals of [Au_2(dcpn)(SC_6H_4F-*p*)$_2$] (100 mg, 0.09 mmol, 81% yield). ^{1}H-NMR (300 MHz, $CDCl_3$, 298 K, relative to Me_4Si): δ 0.86–1.76 (m, 40 H, cyclohexyl), 2.35 (m, 4 H, cyclohexyl), 6.79 (d, 4 H, SC_6H_4), 7.54–7.68 (m, 4 H, SC_6H_4; 2 H, Np) and 7.80–8.06 (m, 4 H, Np). Positive-ion FAB mass spectrum: m/z 1042 {[M–SC_6H_4F-*p*]$^+$}. Elemental analysis: Anal. Found: C, 47.13; H, 5.02. Calc. for $C_{46}H_{58}Au_2F_2P_2S_2$: C, 47.28; H, 4.96%.

*2.2.8. [Au_2(dcpn)(SC_6H_4Cl-*p*)$_2$] (**14**)*

The procedure was similar to that for **13** except 4-chlorothiophenol (31 mg, 0.21 mmol) was used in place of 4-fluorothiophenol. Recrystallization of the crude product gave **14** as orange crystals (103 mg, 0.09 mmol, 81% yield). ^{1}H-NMR (300 MHz, $CDCl_3$, 298 K, relative to Me_4Si): δ 0.70–1.72 (m, 40 H, cyclohexyl), 2.30 (m, 4 H, cyclohexyl), 7.05 (d, 4 H, SC_6H_4), 7.54–7.64 (m, 4 H, SC_6H_4; 2 H, Np) and 7.78–8.04 (m, 4 H, Np). Positive-ion FAB mass spectrum: *m*/*z* 1058 {[M–SC_6H_4Cl-*p*]$^+$}. Elemental analysis: Anal. Found: C, 45.93; H, 4.82. Calc. for $C_{46}H_{58}Au_2Cl_2P_2S_2$: C, 45.98; H, 4.83%.

*2.2.9. [Au_2(dcpn)(SC_6H_4Me-*p*)$_2$] (**15**)*

The procedure was similar to that for **13** except *p*-thiocresol (26 mg, 0.21 mmol) was used in place of 4-fluorothiophenol. Recrystallization of the crude product gave **15** as orange crystals (100 mg, 0.09 mmol, 82% yield). ^{1}H-NMR (300 MHz, $CDCl_3$, 298 K, relative to Me_4Si): δ 0.72–1.76 (m, 40 H, cyclohexyl), 2.30 (m, 4 H, cyclohexyl; 6 H, Me group of SC_6H_4Me), 6.90 (d, 4 H, SC_6H_4), 7.52–7.62 (m, 4 H, SC_6H_4; 2 H, Np) and 7.78–8.02 (m, 4 H, Np). Positive-ion FAB mass spectrum: *m*/*z* 1038 {[M–SC_6H_4Me-*p*]$^+$}. Elemental analysis: Anal. Found: C, 49.63; H, 5.52. Calc. for $C_{48}H_{64}Au_2P_2S_2$: C, 49.68; H 5.51%.

*2.2.10. [Au_2(dcpn)(*S*-benzo-15-crown-5)$_2$] (**16**)*

The procedure was similar to that for **13** except 4′-mercaptomonobenzo-15-crown-5 (64 mg, 0.21 mmol) was used in place of 4-fluorothiophenol. Recrystallization of the crude product gave **16** as a yellow solid (125 mg, 0.08 mmol, 78% yield). ^{1}H-NMR (300 MHz, $CDCl_3$, 298 K, relative to Me_4Si): δ 0.76–1.74 (m, 40 H, cyclohexyl), 2.36 (m, 4 H, cyclohexyl), 3.50–4.02 (m, 32 H, CH_2 of crown ether), 6.55–7.18 (m, 6 H, Ar–H) and 7.52–8.00 (m, 6 H, Np). Positive-ion FAB mass spectrum: *m*/*z* 1513 {M$^+$}. Elemental analysis: Anal. Found: C, 47.51; H, 5.73. Calc. for $C_{62}H_{88}Au_2O_{10}P_2S_2{\cdot}CH_2Cl_2$: C, 47.36; H, 5.63%.

*2.2.11. [Au_2(dcpn){$SC_6H_3(OMe)_2$-3,4}$_2$] (**17**)*

The procedure was similar to that for **13** except 3,4-dimethoxythiophenol (36 mg, 0.21 mmol) was used in place of 4-fluorothiophenol. Recrystallization of the crude product gave **17** as a yellow solid (102 mg, 0.08 mmol, 77% yield). ^{1}H-NMR (300 MHz, $CDCl_3$, 298 K, relative to Me_4Si): δ 0.70–1.74 (m, 40 H, cyclohexyl), 2.30 (m, 4 H, cyclohexyl), 3.80 (m, 12 H, OCH_3), 6.58–7.00 (m, 6 H, Ar–H) and 7.54–7.88 (m, 6 H, Np). Positive-ion FAB mass spectrum: *m*/*z* 1253 {M$^+$}. Elemental analysis: Anal. Found: C, 47.85; H, 5.49. Calc. for $C_{50}H_{68}Au_2O_4P_2S_2$: C, 47.95; H, 5.43%.

2.3. Physical measurements and instrumentation

UV–vis spectra were obtained on a Hewlett–Packard 8452A diode array spectrophotometer, and steady-state excitation and emission spectra on a Spex Fluorolog 111 spectrofluorometer. Low-temperature (77 K) spectra were recorded by

using an optical Dewar sample holder. ^{1}H-NMR spectra were recorded on a Bruker DPX-300 Fourier-transform NMR spectrometer. Positive ion FAB mass spectra were recorded on a Finnigan MAT95 mass spectrometer. Electrospray-ionization mass spectra (ESI-MS) were recorded on a Finnigan MAT LCQ mass spectrometer. Elemental analyses of the new complexes were performed by Butterworth Laboratories Ltd. or the Institute of Chemistry at the Chinese Academy of Sciences in Beijing.

Emission lifetime measurements were performed using a conventional laser system. The excitation source was the 355-nm output (third harmonic) of a Quanta-Ray Q-switched GCR-150-10 pulsed Nd–YAG laser. Luminescence decay signals were recorded on a Tektronix model TDS 620A digital oscilloscope and analyzed using a program for exponential fits. All solutions for photophysical studies were prepared in a 10-cm^3 round-bottomed flask equipped with a side-arm 1-cm fluorescence cuvette and sealed from the atmosphere with a Rotaflo HP6/6 quick-release Teflon stopper. Solutions were rigorously degassed with no fewer than four freeze–pump–thaw cycles.

2.4. Binding studies

The electronic absorption spectral titration for binding constant determination was performed with a Hewlett–Packard 8452A diode array spectrophotometer at 25°C which was controlled by a Lauda RM6 compact low-temperature thermostat. Supporting electrolyte (0.1 mol dm^{-3} ^{n}Bu$_4$NPF$_6$) was added to maintain a constant ionic strength of the sample solution in order to avoid any changes arising from a change in the ionic strength of the medium. Binding constants were determined by a plot of $[A_0/(A_0 - A)]$ or $[I_0/(I_0 - I)]$ against $[\mathrm{M}]^{-1}$ for a 1:1 binding model, from which a straight line plot could be obtained in which the stability constant for the ion-binding is given by the ratio of y-intercept/slope according to Eqs. (1) and (2) [47]:

$$\frac{A_0}{A_0 - A} = \frac{\varepsilon_0}{\varepsilon_0 - \varepsilon}\left[1 + \frac{1}{[\mathrm{M}]K_s}\right] \tag{1}$$

where A_0 and A are the absorbance observed in the absence and presence of M, respectively, and ε_0 and ε are the extinction coefficients for the free and metal ion-bound gold(I) complex.

$$\frac{I_0}{I_0 - I} = \frac{\varepsilon_0 \Phi_0}{\varepsilon_0 \Phi_0 - \varepsilon \Phi}\left[1 + \frac{1}{[\mathrm{M}]K_s}\right] \tag{2}$$

where I_0 and I are the emission intensity observed in the absence and presence of M, respectively, and Φ_0 and Φ are the quantum yields for the free and metal ion-bound gold(I) complex.

3. Results and discussion

3.1. Syntheses and characterization

The dithiolatogold(I) phosphine complexes were prepared by reactions of the corresponding dichlorogold(I) phosphine complexes with arenethiolates generated in situ from the arenethiol and triethylamine as the base. Similar synthetic routes were employed for the preparation of analogous thiolatogold(I) phosphine complexes using bases such as KOH and ethanolamine [6,21]. All the dithiolatodigold(I) phosphine complexes were isolated as a yellow to orange crystals and are stable in both the solid state and in solutions. All the newly synthesized complexes gave satisfactory elemental analyses and have been characterized by ^{1}H-NMR spectroscopy and positive-ion FAB mass spectrometry. The structure of **1** has been determined by X-ray crystallography and was reported previously [10]. A Au···Au separation of 3.4379(4) Å has been observed, indicative of the absence of gold–gold interactions although the bis(diphenylphosphino)amine ligand has a bite distance within separations well suited for short Au···Au contacts to exist [P(1)···P(2) 2.87 Å]. The absence of short Au···Au and S···S contacts [S(1)···S(2) 5.75 Å] as well as the highly unsymmetrical structure of **1** are suggested to be a consequence of the steric requirements of the ligands.

3.2. Electronic absorption and emission spectroscopy

The electronic absorption spectra of the bis(diphenylphosphino)amine-containing complexes **1**–**12** show low energy absorption bands at ca. 365–388 nm, which are absent in the spectra of the corresponding dichlorodigold(I) precursors. Table 1 summarizes the electronic absorption spectral data of complexes **1**–**17**. It is likely that such absorption bands are characteristic of the gold(I) thiolate moiety. A close scrutiny of the absorption spectral data showed that for complexes with the same diphosphine ligand, the absorption energies are lowest for the complexes with the most electron rich 3,4-dimethoxybenzenethiolate ligand, while the absorption band for the 4-chlorobenzenethiolate complexes occurred at highest energy. An absorption energy trend for $[Au_2(Ph_2PN(R)PPh_2)(SR')_2]$ with $R' = C_6H_4Cl$-*p* > C_6H_4F-*p* > C_6H_4Me-*p* > benzo-15-crown-5 ≈ $C_6H_3(OMe)_2$-3,4 has been observed, in line with the σ-donating ability of the thiolate ligands. This low-energy absorption band has been assigned to a thiolate-to-gold LMCT transition, given the better σ-donor ability of the thiolate ligand relative to the chloro group. Similar assignments have been made in analogous gold(I) thiolate [6,8,10,21,30,32]. The anomalous absorption energy trend observed for the fluoro-substituted benzenethiolate complexes has been ascribed to the opposing inductive and mesomeric effect of the fluoro-group, which is commonly observed in other related systems [48,49]. The high energy absorptions at ca. 262–305 nm, which are also present in the chloro analogues, are tentatively assigned as intraligand transitions characteristic of the diphosphine ligands.

For the dcpn-containing complexes **13**–**17**, the electronic absorption spectra reveal high energy absorption bands at ca. 290–320 nm and a lower energy absorption shoulders at ca. 384 nm with tails extending to ca. 500 nm (Table 1). In the case of $[Au_2(dcpn)(S\text{-benzo-15-crown-5})_2]$ (**16**) and $[Au_2(dcpn)\{SC_6H_3(OMe)_2\text{-}3,4\}_2]$ (**17**), the electronic absorption spectra are dominated by the intense high energy absorption band with the low energy shoulders being almost indiscernible. Since the free dcpn ligand shows an intense absorption at ca. 300 nm, the high energy absorption band of complexes **13**–**17** is tentatively assigned as $\pi \rightarrow \pi^*$ intraligand transition within the naphthyl core.

Excitation of solid sample and fluid solution of the dithiolatodigold(I) complexes with visible light at r.t. and at 77 K results in intense luminescence. The photophysical data are collected in Table 2. At r.t., the solid state and fluid solution emission spectra of complexes **1**–**12** are dominated by a broad and intense blue–green emission, typical of metal perturbed ligand-centred emission of the phosphine ligand. However, upon excitation of the solid sample at 77 K, the shape of the emission band becomes highly unsymmetrical; some of which could be resolved into two broad bands, a higher energy one in the blue–green region similar to that observed at r.t. and a lower energy band in the orange. This becomes even more obvious for the 77 K emissions in $CHCl_3$ glass matrices (Fig. 1). Such dual emissive behaviour is suggestive of two closely lying emissive states of different origins. The excitation spectra of the complexes monitored at the low energy emission band at ca. 600 nm show excitation bands at ca. 440 nm, while those monitored at ca. 500 nm show bands at ca. 300–360 nm (Fig. 2). This is in agreement with the

Table 1
Electronic absorption spectral data of $[Au_2(P\text{–}P)(SR)_2]$ (**1–17**) in dichloromethane at 298 K

Complex	P–P	R	Absorption λ (nm) (ε ($dm^3\ mol^{-1}\ cm^{-1}$))
1 [a]	$(Ph_2P)_2NC_6H_{11}$	C_6H_4F-4	278 sh (23 310), 304 sh (14 620), 372 sh (2480)
2 [a]	$(Ph_2P)_2NC_6H_{11}$	C_6H_4Cl-4	280 sh (29 950), 298 sh (24 450), 364 sh (3360)
3 [a]	$(Ph_2P)_2NC_6H_{11}$	$C_6H_4CH_3$-4	276 sh (28 270), 304 sh (15 130), 380 sh (1550)
4 [a]	$(Ph_2P)_2NC_6H_5$	$C_6H_4CH_3$-4	276 sh (22 590), 298 sh (14 620), 382 sh (1810)
5 [a]	$(Ph_2P)_2NC_3H_7$	$C_6H_4CH_3$-4	264 sh (29 920), 298 sh (22 970), 378 sh (4270)
6 [a]	$(Ph_2P)_2NCH(CH_3)_2$	$C_6H_4CH_3$-4	268 sh (26 880), 300 sh (19 310), 382 sh (3130)
7	$(Ph_2P)_2NC_6H_{11}$	Benzo-15-crown-5	268 sh (31 870), 302 sh (19 520), 384 sh (1800)
8	$(Ph_2P)_2NC_6H_{11}$	$C_6H_3(OMe)_2$-3,4	266 sh (25 510), 304 sh (15 040), 388 sh (1510)
9	$(Ph_2P)_2NC_6H_5$	Benzo-15-crown-5	262 sh (31 170), 300 sh (20 290), 388 sh (2770)
10	$(Ph_2P)_2NC_6H_5$	$C_6H_3(OMe)_2$-3,4	264 sh (33 210), 294 sh (22 330), 388 sh (3000)
11	$(Ph_2P)_2NC_3H_7$	Benzo-15-crown-5	262 sh (32 530), 296 sh (23 980), 384 sh (3440)
12	$(Ph_2P)_2NC_3H_7$	$C_6H_3(OMe)_2$-3,4	262 sh (28 700), 296 sh (20 600), 388 sh (2810)
13	dcpn	C_6H_4F-4	290 sh (20 630), 316 sh (14 830), 384 sh (1110)
14	dcpn	C_6H_4Cl-4	292 sh (27 830), 318 sh (17 810), 384 sh (1000)
15	dcpn	C_6H_4Me-4	290 sh (21 480), 324 sh (10 840), 384 sh (1150)
16	dcpn	Benzo-15-crown-5	292 sh (17 970)
17	dcpn	$C_6H_3(OMe)_2$-3,4	292 sh (27 450)

[a] From Ref. [10].

assignment that the 500-nm emission arises from states derived from the metal perturbed intraligand (IL) transitions. The involvement of a phenyl localized $^3\pi\pi^*$ origin on the phosphine ligands is probable since similar emissions have also been reported in other related gold(I) systems [50–52]. It is likely that the low energy emissions at ca. 600 nm, which are absent for the chlorogold(I) counterparts, originate from emissive states derived from thiolate-to-gold LMCT transitions. The large Stokes shifts together with the observed lifetimes in the microsecond range are suggestive of a triplet parentage. The 440 nm excitation band, which in the electronic absorption spectrum of **5**, appears as a very weak tail and is possibly obscured by the more intense absorption bands, is tentatively assigned to be derived from a ^{3}LMCT origin, and associated with the phosphorescence at 600 nm. Further support for an LMCT origin comes from the observed trends in emission energies upon variation of the thiolate ligands. $[Au_2(Ph_2PN(C_6H_{11})PPh_2)(SC_6H_4F\text{-}p)_2]$ (**1**) and $[Au_2(Ph_2PN(C_6H_{11})PPh_2)(SC_6H_4Cl\text{-}p)_2]$ (**2**) are found to emit at higher energies than $[Au_2(Ph_2PN(C_6H_{11})PPh_2)(SC_6H_4Me\text{-}p)_2]$ (**3**), in line with an assignment involving states derived from a LMCT transition, where the σ-donor ability of the thiolate moiety containing tolyl substituent is expected to be the highest amongst the three (Fig. 3). On pure electronic grounds, the fluoro-substituted thiolate should be a poorer σ-donor than its chloro counterpart. Thus the anomalously lower emission energy in $[Au_2(Ph_2PN(C_6H_{11})PPh_2)(SC_6H_4F\text{-}p)_2]$ (**1**) relative to $[Au_2(Ph_2PN(C_6H_{11})PPh_2)(SC_6H_4Cl\text{-}p)_2]$ (**2**) probably arises as a result of the stronger mesomeric effect of the fluoro substituent which increases the electron density on the sulfur atom through π donation into its empty 3d orbital. Similar observations have been reported in ^{31}P-NMR spectroscopic studies of fluoro-substituted phosphines [48,49]. With the complexes $[Au_2(Ph_2PN(R)PPh_2)(SC_6H_4Me\text{-}p)_2]$, where R = C_6H_{11}, Ph, ^{n}Pr and ^{i}Pr, the low energy emissions are relatively insensitive to the nature of the bis(diphenylphosphino)amine ligands. The slightly lower emission energy for $[Au_2(Ph_2PN(Ph)PPh_2)(SC_6H_4Me\text{-}p)_2]$ (**4**) may be accounted for by the presence of the less electron rich $Ph_2PN(Ph)PPh_2$ ligand, which renders the gold(I) centres more electron deficient and hence lowers the metal acceptor-orbital energy. Although the possibility of a thiolate to phosphine ligand-to-ligand charge transfer (LLCT) transition as the origin of the low-energy emission cannot be excluded, the assignment of a LMCT origin is still favoured based on the following grounds. First, only a small dependence of emission energies on the nature of the diphosphine ligand is observed. An emission of LLCT origin should give rise to a much larger energy dependence. Secondly, spectroscopic studies on other similar gold(I) thiolate systems have also confirmed a LMCT origin for the emission [6,8,10,21,30,32]. A LMMCT origin which has been suggested to operate in the solid state emission of some gold(I) thiolate complexes [6] is unlikely in the present complexes since there is no evidence of gold–gold interactions of any kind, neither intra- nor inter-molecular in nature.

Excitation of solid samples of the dcpn-containing complexes **13**–**17** at $\lambda > 350$ nm produces intense luminescence (Table 2). The spectra of $[Au_2(dcpn)(SC_6H_4F\text{-}p)_2]$ (**13**), $[Au_2(dcpn)(SC_6H_4Cl\text{-}p)_2]$ (**14**) and $[Au_2(dcpn)(SC_6H_4Me\text{-}p)_2]$ (**15**) all show a single structureless band at 637, 626 and 630 nm, respectively. The luminescence

Table 2
Photophysical data of complexes $[Au_2(P–P)(SR)_2]$ (**1–17**)

Complex	P–P	R	Medium (T (K))	Emission λ (nm) (τ_0 (μs))
1 [a]	$(Ph_2P)_2NC_6H_{11}$	C_6H_4F-4	Solid (298)	519 (0.18, 0.77) [b]
			Solid (77)	540
			CH_2Cl_2 (298)	503 (<0.1)
			$CHCl_3$ (77)	488, 567
2 [a]	$(Ph_2P)_2NC_6H_{11}$	C_6H_4Cl-4	Solid (298)	513 (0.64, 3.6) [b]
			Solid (77)	528
			CH_2Cl_2 (298)	499 (<0.1)
			$CHCl_3$ (77)	485, 545
3 [a]	$(Ph_2P)_2NC_6H_{11}$	$C_6H_4CH_3$-4	Solid (298)	519, 552 (0.19, 0.81) [b]
			Solid (77)	522, 590
			CH_2Cl_2 (298)	503 (<0.1)
			$CHCl_3$ (77)	498, 607
4 [a]	$(Ph_2P)_2NC_6H_5$	$C_6H_4CH_3$-4	Solid (298)	506 (0.28)
			Solid (77)	508, 578
			CH_2Cl_2 (298)	518 (<0.1)
			$CHCl_3$ (77)	495, 618
5 [a]	$(Ph_2P)_2NC_3H_7$	$C_6H_4CH_3$-4	Solid (298)	530 (0.11, 0.45) [b]
			Solid (77)	525, 602
			CH_2Cl_2 (298)	557 (<0.1)
			$CHCl_3$ (77)	495, 602
6 [a]	$(Ph_2P)_2NCH(CH_3)_2$	$C_6H_4CH_3$-4	Solid (298)	517 (0.29, 1.4) [b]
			Solid (77)	520, 609
			CH_2Cl_2 (298)	540 (<0.1)
			$CHCl_3$ (77)	493, 604
7	$(Ph_2P)_2NC_6H_{11}$	Benzo-15-crown-5	Solid (298)	575 (0.69)
			Solid (77)	538, 589
			CH_2Cl_2 (298)	571 (<0.1)
			$CHCl_3$ (77)	505, 608
8	$(Ph_2P)_2NC_6H_{11}$	$C_6H_3(OMe)_2$-3,4	Solid (298)	576 (0.63)
			Solid (77)	529, 591
			CH_2Cl_2 (298)	552 (<0.1)
			$CHCl_3$ (77)	504, 571
9	$(Ph_2P)_2NC_6H_5$	Benzo-15-crown-5	Solid (298)	567, 616 (0.62)
			Solid (77)	544, 622
			CH_2Cl_2 (298)	596 (<0.1)
			$CHCl_3$ (77)	507, 615
10	$(Ph_2P)_2NC_3H_7$	$C_6H_3(OMe)_2$-3,4	Solid (298)	554, 606 (0.64)
			Solid (77)	554, 643
			CH_2Cl_2 (298)	586 (<0.1)
			$CHCl_3$ (77)	506, 579
11	$(Ph_2P)_2NC_3H_7$	Benzo-15-crown-5	Solid (298)	586 (0.96, 1.36) [b]
			Solid (77)	560, 604
			CH_2Cl_2 (298)	591 (<0.1)
			$CHCl_3$ (77)	509, 613

Table 2 (*Continued*)

Complex	P–P	R	Medium (T (K))	Emission λ (nm) (τ_0 (μs))
12	$(Ph_2P)_2NC_3H_7$	$C_6H_3(OMe)_2$-3,4	Solid (298)	579 (0.50)
			Solid (77)	545, 619
			CH_2Cl_2 (298)	602 (<0.1)
			$CHCl_3$ (77)	497, 601
13	dcpn	C_6H_4F-4	Solid (298)	637 (<0.1)
			Solid (77)	652
			CH_2Cl_2 (298)	510, 545 sh (<0.1)
			$CHCl_3$ (77)	629
14	dcpn	C_6H_4Cl-4	Solid (298)	626 (<0.1)
			Solid (77)	644
			$CHCl_3$ (77)	614
15	dcpn	C_6H_4Me-4	Solid (298)	630 (<0.1)
			Solid (77)	640
			$CHCl_3$ (77)	627
16	dcpn	Benzo-15-crown-5	Solid (298)	621 (0.11)
			Solid (77)	660
			CH_2Cl_2 (298)	512, 559 sh (<0.1)
			$CHCl_3$ (77)	626
17	dcpn	$C_6H_3(OMe)_2$-3,4	Solid (298)	629 (<0.1)
			Solid (77)	645
			$CHCl_3$ (77)	628

[a] From Ref. [10].
[b] The lifetimes measured showed a bi-exponential decay.

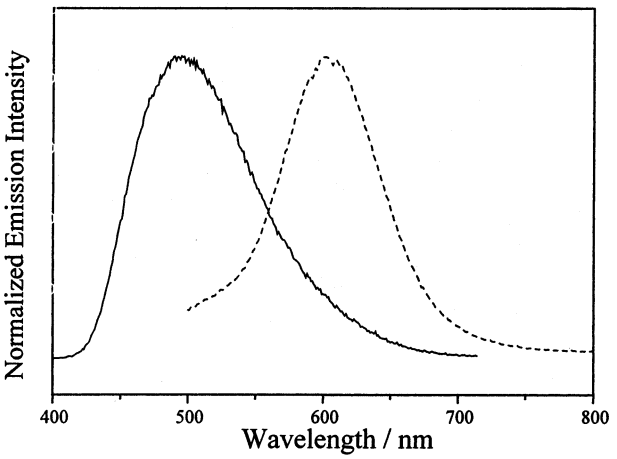

Fig. 1. Normalized emission spectra of **5** as a 77 K $CHCl_3$ glass excited at 300 (—) and 440 nm (---). Reproduced with permission from Ref. [10].

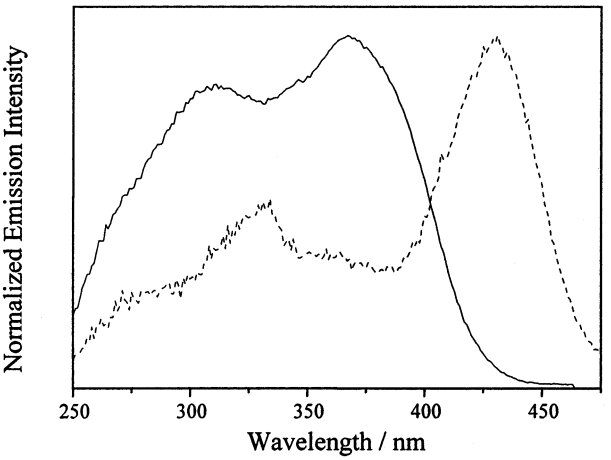

Fig. 2. Normalized excitation spectra of **5** as a 77 K $CHCl_3$ glass monitored at $\lambda = 500$ (—) and 650 nm (---). Reproduced with permission from Ref. [10].

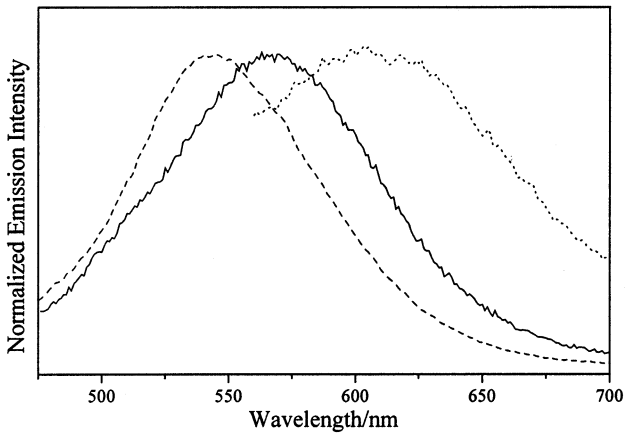

Fig. 3. Normalized emission spectra of **1** (—), **2** (---) and **3** (·····) as a 77 K $CHCl_3$ glass excited at $\lambda = 440$ nm.

lifetimes monitored at the emission maxima of these complexes are in the microsecond range, suggesting that the emissions are phosphorescence in nature. Emissions in degassed dichloromethane solution at ambient temperature can only be obtained for $[Au_2(dcpn)(SC_6H_4F\text{-}p)_2]$ (**13**) and $[Au_2(dcpn)(S\text{-benzo-15-crown-5})_2]$ (**16**). For the 77 K emissions in $CHCl_3$ glass matrices, the spectra of $[Au_2(dcpn)(SC_6H_4F\text{-}p)_2]$ (**13**), $[Au_2(dcpn)(SC_6H_4Cl\text{-}p)_2]$ (**14**) and $[Au_2(dcpn)(SC_6H_4Me\text{-}p)_2]$ (**15**) all show a single structureless band centred at 629, 614 and 627 nm, respectively.

The emissions in the solid state and in glass matrices at 77 K are probably derived from the same origin. The 77 K-glass emission energies of $[Au_2(dcpn)(SR)_2]$

follow the order: C_6H_4Cl-*p* > benzo-15-crown-5 ≈ C_6H_4Me-*p* ≈ $C_6H_3(OMe)_2$-3,4 ≈ C_6H_4F-*p*. This observation was in line with the assignment of an emissive origin derived from states of a LMCT transition since attachment of electron-withdrawing groups on the benzenethiolate ligands caused a blue shift of the emission energy. Again, the anomalous emission energy trend observed for the fluoro-substituted benzenethiolate complex is consistent with the opposing inductive and mesomeric effect of the fluoro-group that is commonly observed in other related systems [48,49].

A red shift in emission energies of the dcpn-containing complexes relative to their corresponding bis(diphenylphosphino)amine-containing counterparts was observed (Fig. 4). For example, the emission of 77 K-$CHCl_3$ glass of **1** and **13** occurred at 567 and 629 nm, respectively. Suppose the excited states are associated with a high parentage of thiolate-to-gold charge-transfer character, the presence of gold–gold interactions would significantly alter the emission energy of the system. The X-ray crystal structure of $[Au_2\{Ph_2PN(C_6H_{11})PPh_2\}(SC_6H_4F\text{-}p)_2]$ (**1**) shows a highly unsymmetrical geometry. Although the bite distance of the $Ph_2PN(C_6H_{11})PPh_2$ ligand is within separations well suited for short Au···Au contacts (P···P = 2.87 Å), a Au···Au separation of 3.4379(4) Å indicates very weak to almost no gold–gold interactions. On the other hand, unlike the bis(diphenylphosphino)amine ligands, the dcpn ligand is a relatively more rigid ligand as the phosphorus atoms are attached to a rigid naphthyl ring (P···P = 3.052 Å for dppn) [44]. When the gold atoms form bonds with the two phosphorus atoms of the dcpn ligand in a bridging fashion, the two gold atoms would be brought into close proximity. As a result, gold–gold interaction would be resulted or enhanced which would destabilize the d_{σ^*} orbital derived from $5d_{z^2}$–$5d_{z^2}$ orbital overlap (the *z*-axis is taken along the metal–metal axis) and stabilize the empty p_σ orbital derived from $6p_z$–$6p_z$ orbital overlap. This would have the net effect of lowering the energy of the LMMCT ($RS^- \rightarrow Au_2$ LMMCT) transition and causing a red shift in the emission energy

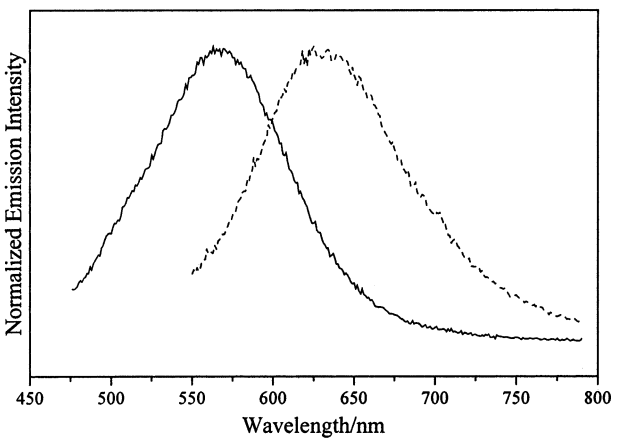

Fig. 4. Normalized emission spectra of **1** (—) and **13** (---) as a 77 K $CHCl_3$ glass excited at $\lambda = 440$ nm.

derived from an emissive origin of such LMMCT state. Thus the assignment of a LMMCT emission origin for the dcpn-containing complexes may be a better description, particularly for the solid-state and low-temperature emissions.

3.3. Binding studies

In view of the rich spectroscopic and luminescence properties of dinuclear Au(I) phosphine thiolate complexes, the ion-binding behaviour of gold(I) complexes with crown ether moieties was explored.

Upon addition of potassium ions to complexes **11** and **16** in dichloromethane/methanol (1:1, v/v) containing 0.1 mol dm^{-3} tetra-*n*-butylammonium hexafluorophosphate as supporting electrolyte, a substantial change in the UV–vis

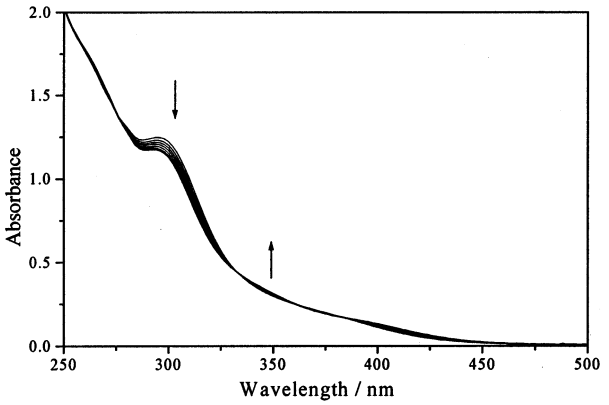

Fig. 5. Electronic absorption spectral traces of **11** in CH_2Cl_2/MeOH (1:1, v/v) containing 0.1 mol dm^{-3} $^nBu_4NPF_6$ upon addition of potassium acetate.

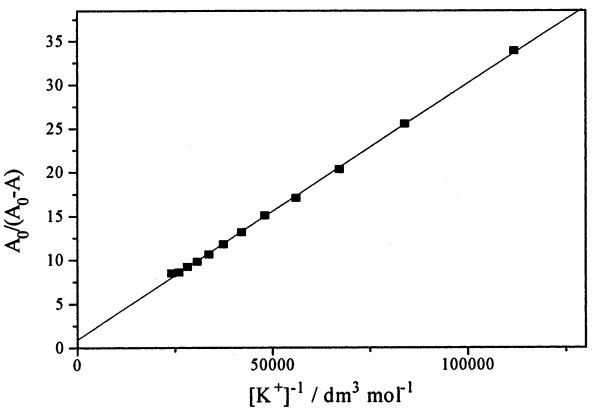

Fig. 6. A plot of $A_0/(A_0 - A)$ vs. $[K^+]^{-1}$ for **11** in CH_2Cl_2/MeOH (1:1, v/v) containing 0.1 mol dm^{-3} $^nBu_4NPF_6$ at 298 K. The absorbance was monitored at 300 nm.

absorption spectrum was observed. The electronic absorption spectral traces of $[Au_2(Ph_2PN(^nPr)PPh_2)(S\text{-benzo-15-crown-5})_2]$ (**11**) upon addition of potassium ions were illustrated in Fig. 5. Clean isosbestic points at 330 and 380 nm were observed in the electronic absorption spectra. For the case of $[Au_2(dcpn)(S\text{-benzo-15-crown-5})_2]$ (**16**), similar isosbestic points appeared at 310 and 365 nm in the electronic absorption spectra. The presence of isosbestic points is an indication of a clean reaction resulted from the addition of potassium ions.

Control experiments with the crown-free analogues $[Au_2(Ph_2PN(^nPr)PPh_2)\text{-}\{SC_6H_3(OMe)_2\text{-}3,4\}_2]$ (**12**) and $[Au_2(dcpn)\{SC_6H_3(OMe)_2\text{-}3,4\}_2]$ (**17**) did not yield any absorption spectral changes upon addition of K^+ ions under the same conditions. This observation is supportive of the importance of the crown moieties in the specific association of $[Au_2(Ph_2PN(^nPr)PPh_2)(S\text{-benzo-15-crown-5})_2]$ (**11**) and $[Au_2(dcpn)(S\text{-benzo-15-crown-5})_2]$ (**16**) with K^+ ions rather than resulting from changes in the solvent polarity.

In order to gain more insight into the cation-binding properties of the complexes, the stability constants of $[Au_2(Ph_2PN(^nPr)PPh_2)(S\text{-benzo-15-crown-5})_2]$ (**11**) and $[Au_2(dcpn)(S\text{-benzo-15-crown-5})_2]$ (**16**) with K^+ ions were determined. The log K_s values for the binding of K^+ ions to the complexes $[Au_2(Ph_2PN(^nPr)PPh_2)(S\text{-benzo-15-crown-5})_2]$ (**11**) and $[Au_2(dcpn)(S\text{-benzo-15-crown-5})_2]$ (**16**) were 4.46 and 4.44, respectively. Linear plots of $[A_0/(A_0 - A)]$ against $[K^+]^{-1}$ for complexes **11** (Fig. 6) and **16** were obtained, indicating that the complexation of a K^+ ion to the dinuclear Au(I) complex was in a 1:1 ratio. Since the ionic radius of the K^+ ion is too large to fit into the cavity of a benzo-15-crown-5, the 1:1 complexation ratio indicates that one K^+ ion is sandwiched between two benzo-15-crown-5 units within the dinuclear Au(I) complex.

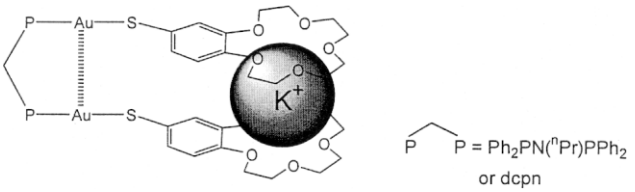

The formation of the 1:1 (K^+:Au_2) sandwich species was directly detected by ESI-MS. The presence of sandwich species was confirmed by the similar isotope pattern of the ion clusters expanded from the mass spectra and that simulated for the sandwich adducts (Figs. 7 and 8).

The cation-binding properties of the analogous dppm and dcpm complexes, $[Au_2(dppm)(S\text{-benzo-15-crown-5})_2]$ and $[Au_2(dcpm)(S\text{-benzo-15-crown-5})_2]$ have recently been reported by us [28]. The complexes exhibited log K_s values of 3.4 and 4.0, respectively, for K^+ ion-binding [28]. The observation of the potassium ion-bound adduct, in which one potassium ion is sandwiched between the two benzo-15-crown-5 rings of the dinuclear Au(I) molecule, has also been confirmed by ESI-MS studies.

The changes in the luminescence response of $[Au_2(dppm)(S\text{-benzo-15-crown-5})_2]$ and $[Au_2(dcpm)(S\text{-benzo-15-crown-5})_2]$ towards K^+ ion binding were found to be

more pronounced [28]. As shown in Fig. 9, the emission spectra of $[Au_2(dppm)(S\text{-benzo-15-crown-5})_2]$ excited at 390 nm (isosbestic wavelength), showed a drop in intensity at ca. 502 nm with the concomitant formation of a new long-lived low-energy emission band at 720 nm upon addition of K^+ ions. An isoemissive point was obtained at ca. 600 nm. An excited state lifetime of 0.2 μs has been observed for the 720 nm emission band. Interestingly, in the absence of K^+ ions,

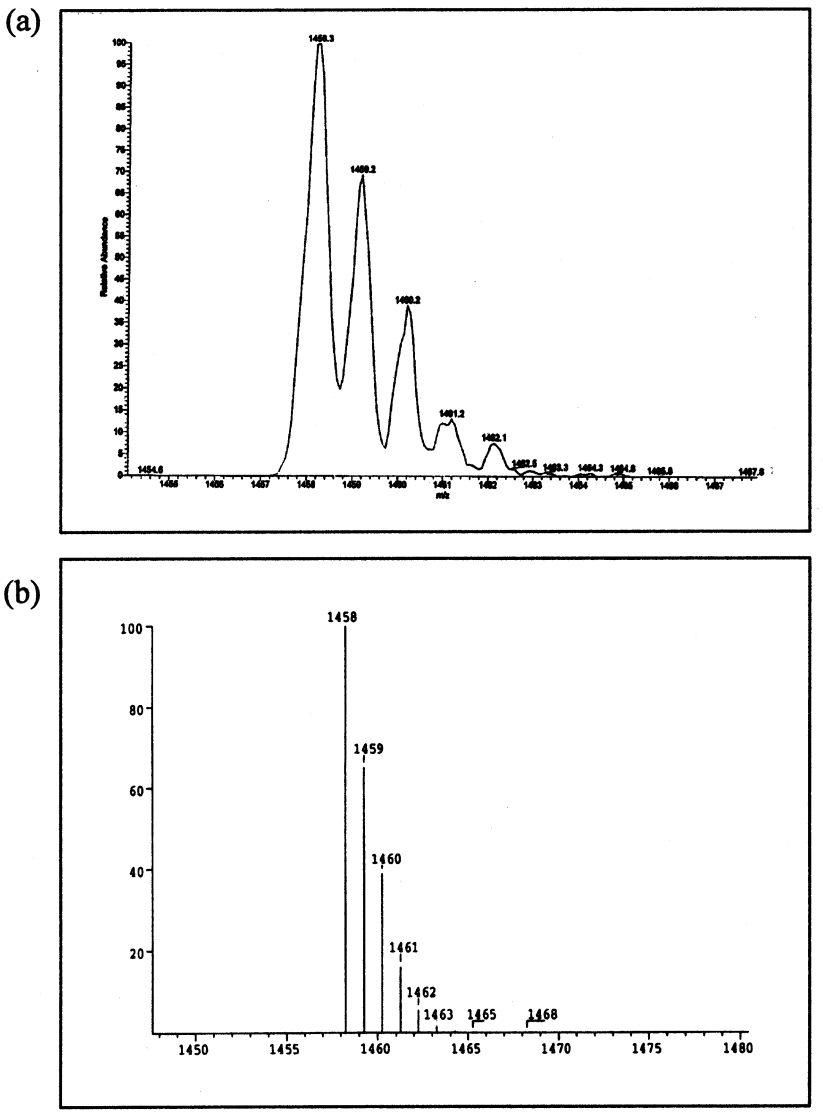

Fig. 7. (a) Ion cluster at m/z 1458, expanded from the positive ESI mass spectrum of a CH_2Cl_2/MeOH solution of **11** and KPF_6. (b) Simulated isotope pattern for the adduct $\{\mathbf{11}\cdot K\}^+$.

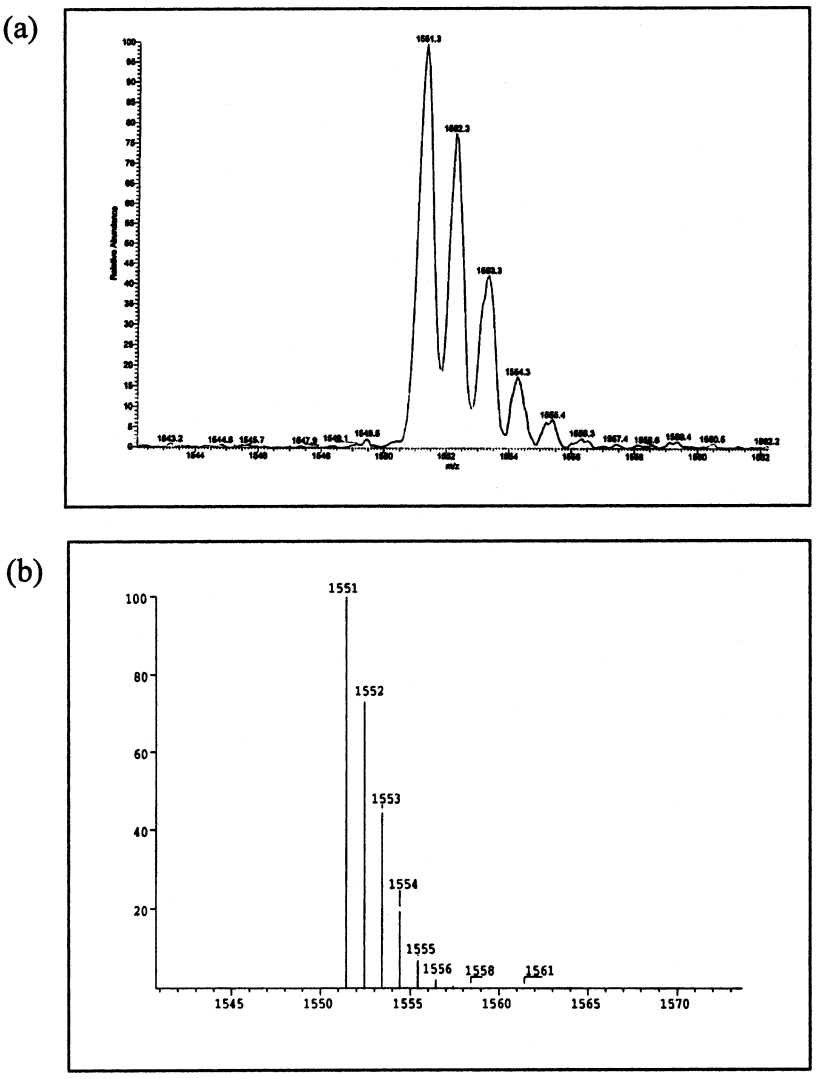

Fig. 8. (a) Ion cluster at m/z 1551, expanded from the positive ESI mass spectrum of a CH_2Cl_2/MeOH solution of **16** and KPF_6. (b) Simulated isotope pattern for the adduct $\{[\mathbf{16}]\cdot K\}^+$.

the emissive lifetime of the 520 nm band was < 0.1 μs. Successive addition of free benzo-15-crown-5 to the mixture of $[Au_2(dppm)(S\text{-benzo-15-crown-5})_2]$ and K^+ ions led to the observation of a reverse trend in which the low-energy emission at 720 nm dropped in intensity concomitant with a rise in the high-energy emission at 502 nm. This is indicative of the reversible nature of the ion-binding process. Similar trend was observed by successive addition of an excess of Na^+ ions to the mixture of $[Au_2(dppm)(S\text{-benzo-15-crown-5})_2]$ and K^+ ions, indicative of the

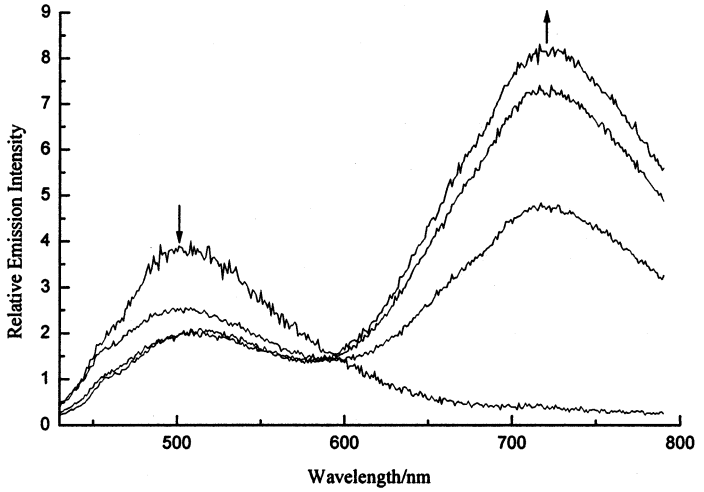

Fig. 9. Emission spectra of $[Au_2(dppm)(S\text{-benzo-15-crown-5})_2]$ upon addition of various concentration of KPF_6 in CH_2Cl_2/MeOH (1/1 v/v; 0.1 M $^nBu_4NPF_6$). Reproduced with permission from Ref. [28].

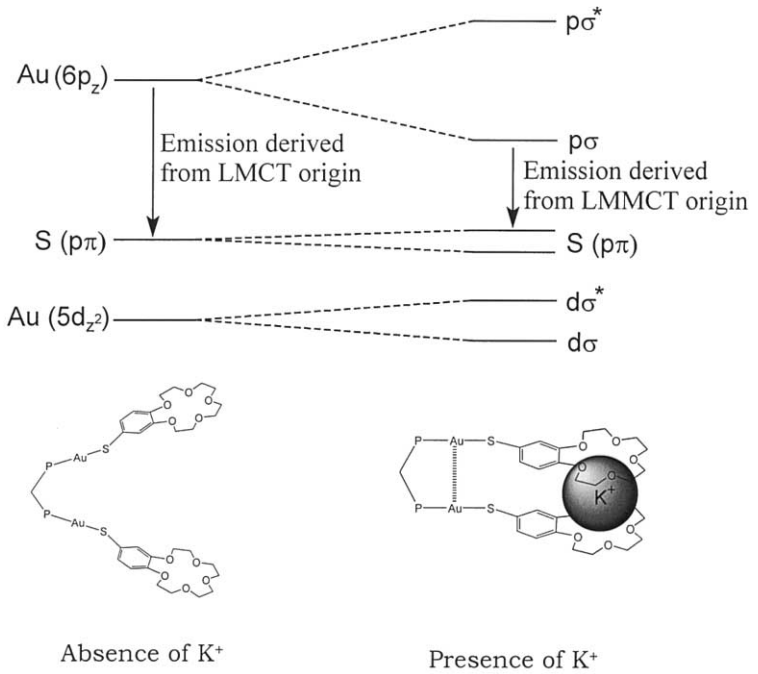

Fig. 10. Schematic representation of the orbital splittings expected with Au···Au interactions in (phosphine)gold thiolates.

competition of Na^+ with K^+ ions for the binding site. The observation of a straight line plot for $I_0/(I_0 - I)$ versus $[K^+]^{-1}$, further confirms that the 1:1 complexation stoichiometry of K^+ ion to the dinuclear Au(I) complex, with a log K_s value of 3.2, which is in close agreement with that obtained from absorption titrations. The identity of the $\{[Au_2(dppm)(S\text{-benzo-15-crown-5})_2]\cdot K^+\}$ adduct was confirmed by ESI-MS. Similar to the absorption studies, control experiments using the crown-free analogues $[Au_2(dppm)\{SC_6H_4(OMe)_2\text{-}3,4\}_2]$ and $[Au_2(dcpm)\{SC_6H_4\text{-}(OMe)_2\text{-}3,4\}_2]$ showed no changes in the emission characteristics upon addition of K^+ ions under the same conditions, supportive of the importance of the crown moieties in the specific association of $[Au_2(dppm)(S\text{-benzo-15-crown-5})_2]$ and $[Au_2(dcpm)(S\text{-benzo-15-crown-5})_2]$ with K^+ ions.

Despite the well-known binding of sodium ions by benzo-15-crown-5 compounds, similar emission spectral changes are not observed when sodium ions are used instead of potassium ions. These observations are in line with our expectations when the benzo-15-crown-5 ring was deliberately chosen in the design of these molecules, in that the cavity size of the benzo-15-crown-5 ring is too small to fit a K^+ ion, forcing its binding to the benzo-15-crown-5 to be in a sandwich binding mode. Thus, it is likely that the binding of K^+ would bring the two gold(I) centres in close proximity to each other, resulting in some weak gold···gold interactions. These intramolecular gold···gold interactions are then reported by the emission properties of the complexes. The low-energy emission band has been proposed to arise from a LMMCT $[RS^- \rightarrow Au_2]$ excited state (Fig. 10).

4. Concluding remarks

This paper summarized our recent efforts on the molecular design of luminescent metal complexes and how one, by the fundamental understanding of the spectroscopic and emission origin of their excited states, could extend the work to the use of selected building blocks for the design of versatile spectrochemical and luminescence chemosensors as well as molecular optoelectronic 'on–off' switching devices. The present system not only serves as a molecular phosphorescent signalling ion sensor and a molecular optoelectronic switch, but also provides spectroscopic evidences for potassium ion induced gold···gold interactions.

Acknowledgements

V.W.W.Y. acknowledges financial support from the Research Grants Council and The University of Hong Kong, and the receipt of a Croucher Senior Research Fellowship from the Croucher Foundation, C.L.C. the receipt of a Croucher Foundation Scholarship administered by the Croucher Foundation and a Sir Edward Youde Postgraduate Scholarship administered by the Sir Edward Youde Memorial Fund Council, C.K.L. the receipt of a University Postgraduate Studentship and K.M.C.W. the receipt of a University Postdoctoral Fellowship, both of which are administered by The University of Hong Kong.

References

[1] D.M.P. Mingos, J. Chem. Soc. Dalton Trans. (1976) 1163.
[2] P.C. Ford, A. Vogler, Acc. Chem. Res. 26 (1993) 220.
[3] P.C. Ford, Coord. Chem. Rev. 132 (1994) 129.
[4] P.C. Ford, E. Cariati, J. Bourassa, Chem. Rev. 99 (1999) 3625.
[5] A. Vogler, H. Kunkely, Chem. Phys. Lett. 150 (1988) 135.
[6] J.M. Forward, D. Bohmann, J.P. Fackler Jr., R.J. Staples, Inorg. Chem. 34 (1995) 6330.
[7] Z. Assefa, B.G. McBurnett, R.J. Staples, J.P. Fackler Jr., B. Assmann, K. Angermaier, H. Schmidbaur, Inorg. Chem. 34 (1995) 75.
[8] H.K. Yip, A. Schier, J. Riede, H. Schmidbaur, J. Chem. Soc. Dalton Trans. (1994) 2333.
[9] V.W.W. Yam, T.F. Lai, C.M. Che, J. Chem. Soc. Dalton Trans. (1990) 3747.
[10] V.W.W. Yam, C.L. Chan, K.K. Cheung, J. Chem. Soc. Dalton Trans. (1996) 4019.
[11] V.W.W. Yam, E.C.C. Cheng, K.K. Cheung, Angew. Chem. Int. Ed. 38 (1999) 197.
[12] V.W.W. Yam, E.C.C. Cheng, Z.Y. Zhou, Angew. Chem. Int. Ed. 39 (2000) 1683.
[13] V.W.W. Yam, W.K. Lee, T.F. Lai, J. Chem. Soc. Chem. Commun. (1993) 1571.
[14] V.W.W. Yam, K.K.W. Lo, Comments Inorg. Chem. 19 (1997) 209.
[15] V.W.W. Yam, K.K.W. Lo, Chem. Soc. Rev. 28 (1999) 323.
[16] V.W.W. Yam, W.K. Lee, T.F. Lai, Organometallics 12 (1993) 2383.
[17] V.W.W. Yam, W.K.M. Fung, K.K. Cheung, Angew. Chem. Int. Ed. Engl. 35 (1996) 1100.
[18] S.J. Shieh, X. Hong, S.M. Peng, C.M. Che, J. Chem. Soc. Dalton Trans. (1994) 3067.
[19] C.M. Che, H.K. Yip, W.C. Lo, S.M. Peng, Polyhedron 13 (1994) 887.
[20] H.R.C. Jaw, M.M. Savas, R.D. Rogers, W.R. Mason, Inorg. Chem. 28 (1989) 1028.
[21] R. Narayanswamy, M.A. Young, E. Parkhurst, M. Ouellette, M.E. Kerr, D.M. Ho, R.C. Elder, A.E. Bruce, M.R.M. Bruce, Inorg. Chem. 32 (1993) 2506.
[22] K.M. Merz Jr., R. Hoffmann, Inorg. Chem. 27 (1988) 2120.
[23] J.V. Caspar, J. Am. Chem. Soc. 107 (1985) 6718.
[24] P.D. Harvey, H.B. Gray, J. Am. Chem. Soc. 110 (1988) 2145.
[25] C. King, J.C. Wang, M.N.I. Khan, J.P. Fackler Jr., Inorg. Chem. 28 (1989) 2145.
[26] V.W.W. Yam, W.K. Lee, J. Chem. Soc. Dalton Trans. (1993) 2097.
[27] V.W.W. Yam, S.W.K. Choi, J. Chem. Soc. Dalton Trans. (1994) 2057.
[28] V.W.W. Yam, C.K. Li, C.L. Chan, Angew. Chem. Int. Ed. 37 (1998) 2857.
[29] C.M. Che, H.L. Kwong, C.K. Poon, V.W.W. Yam, J. Chem. Soc. Dalton Trans. (1990) 3215.
[30] W.B. Jones, J. Yuan, R. Narayanswamy, M.A. Young, R.C. Elder, A.E. Bruce, M.R.M. Bruce, Inorg. Chem. 34 (1995) 1996.
[31] M. Henary, J.I. Zink, J. Am. Chem. Soc. 111 (1989) 7407.
[32] S.D. Hanna, J.I. Zink, Inorg. Chem. 35 (1996) 297.
[33] R.F. Ziolo, S. Lipton, Z. Dori, J. Chem. Soc. Chem Commun. (1970) 1124.
[34] J.P. Fackler Jr., Prog. Inorg. Chem. 21 (1976) 55.
[35] H. Schmidbaur, Chem. Soc. Rev. 24 (1995) 391.
[36] P. Pyykkö, Chem. Rev. 97 (1997) 597.
[37] V.W.W. Yam, P.K.Y. Yeung, K.K. Cheung, Angew. Chem. Int. Ed. Engl. 35 (1996) 739.
[38] R.B. King, Acc. Chem. Res. 13 (1980) 243.
[39] R. Keat, L.M. Muir, K.W. Muir, D.S. Rycroft, J. Chem. Soc. Dalton Trans. (1981) 2192.
[40] H.J. Chen, J.F. Barendt, R.C. Haltiwanger, T.G. Hill, A.D. Norman, Phosphorus Sulfur 26 (1986) 155.
[41] W. Wiegräbe, H. Bock, Chem. Ber. 101 (1968) 1414.
[42] R.J. Cross, T.H. Green, R. Keat, J. Chem. Soc. Dalton Trans. (1976) 1424.
[43] J. Ellermann, L. Mader, Spectrochim. Acta 37A (1981) 449.
[44] R.D. Jackson, S. James, A.G. Orpen, P.G. Pringle, J. Organomet. Chem. 458 (1993) C3.
[45] S. Shinkai, T. Minami, Y. Araragi, O. Manabe, J. Chem. Soc. Perkin Trans. II (1985) 503.
[46] H. Schmidbaur, F.E. Wagner, A. Wohlleben-Hammer, Chem. Ber. 112 (1979) 496.

[47] S. Fery-Forgues, M.T. Le Bris, J.P. Ginette, B. Valeur, J. Phys. Chem. 92 (1988) 6233.
[48] K. Seyferth, R. Taube, J. Organomet. Chem. 229 (1982) C19.
[49] N. Zhang, C.M. Mann, P.A. Shapley, J. Am. Chem. Soc. 110 (1988) 6591.
[50] D.V. Toronto, B. Weissbart, D.S. Tinti, A.L. Balch, Inorg. Chem. 35 (1996) 2484.
[51] L.J. Larson, E.M. McCauley, B. Weissbart, D.S. Tinti, J. Phys. Chem. 99 (1995) 7218.
[52] B. Weissbart, D.V. Toronto, A.L. Balch, D.S. Tinti, Inorg. Chem. 35 (1996) 2490.